Earthquake Engineering, Tenth World Conference © 1992 Balkema, Rotterdam. ISBN 90 5410 060 5

Development of seismic isolation system for light equipment using friction pendulum bearings

Y. Morikawa
Graduate School of Tokyo Denki University, Japan

S. Fujita
Tokyo Denki University, Japan

S. Nagata & I. Shimoda
Oiles Corporation, Japan

ABSTRACT: The friction pendulum bearing developed in this program has a very simple construction for seismic isolator. It only consists of an articulated friction slider which moves on a spherical concave surface and provides the supported equipment a designed frequency obtained by a radius of curvature and gravity. And the articulated friction slider dissipates energy as a friction damper. In this paper we conducted shaking table tests and theoretical analysis in order to investigate the performance of isolation and the restoring force characteristics of the earthquake isolation system using the friction pendulum bearings. It was confirmed that this isolation system is very much effective for reducing response acceleration of equipment due to seismic excitation.

1 INTRODUCTION

During the last few years as we enter a new era of a high level of information-oriented society, the number of buildings having multi-functions has been increasing. Seismic isolation technology can protect not only the structural elements of a building but also its primary function from destructive earthquake motion. It is with such background that many types of earthquake isolation floor or system have been already developed and widespread in Japan (Fujita 1991).

Almost all isolation floors/systems developed especially for critical equipment such as computer systems so far consist of coil springs to provide equipment a designed natural frequency and energy absorbing devices such as friction dampers and oil dampers. However these types of earthquake isolation floor or system may become expensive although they perform satisfactorily.

The friction pendulum bearings developed in this program would solve this problem (Shimoda 1990). This device consists of an articulated friction slider which moves on a spherical concave surface and provides the supported equipment a designed frequency obtained by a radius of curvature and gravity. And the articulated friction slider dissipates energy as a friction damper. In this paper we conducted shaking table tests and theoretical analysis in order to investigate the performance of isolation and the restoring force characteristics of the earthquake isolation system using the friction pendulum bearings.

2 SHAKING TABLE TESTS

2.1 Structure of the friction pendulum bearing

The friction pendulum bearing, which expresses the FPB after this, is a friction pendulum that applies principles of pendulum motion. Figure 1 shows the schematic view of the FPB, which is composed of the upper device made of an articulated friction slider and a Teflon bearing material and the lower device made of a spherical concave surface of stainless steel. By selecting the radius of curvature of the spherical concave and a friction coefficient of the bearing material properly, an optional characteristic period and a friction force can be realized fundamentally.

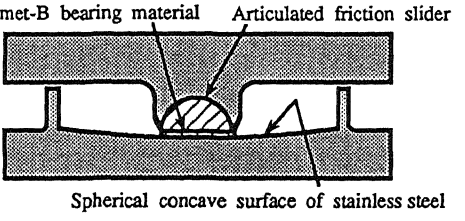

Fig. 1 Schematic view of the friction pendulum bearing

2.2 Test model, equipment and method

In order to examine the dynamic properties and the performance of isolation of the device, dynamic tests were carried out for two computers, whose mass is 130 kg and 78 kg respectively, supported by the four full-size FPB using a shaking table at Meiji University as shown in Fig. 2 and Fig. 3. The FPB was designed to provide a superstructure with a horizontal natural period of 2 s (radius of curvature is 993 mm) and to accept a horizontal displacement of 200 mm. For the friction element to absorb energy, Teflon material called Oiles Techmet-B was used. This material was chosen because of having an advantageous characteristic, which the friction coefficient increases as the relative velocity increases as shown in Fig. 6.

The two-dimensional shaking table tests for seismic waves were carried out. In the tests, the horizontal and

Fig. 2 Test apparatus

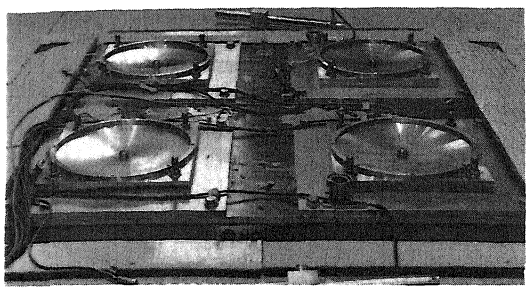

Fig.3 The FPB set up on the shaking table

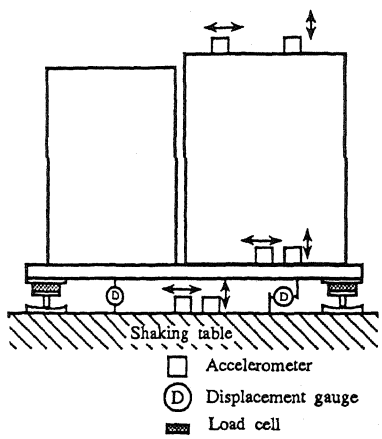

Fig. 4 Schematic view of isolated equipment and measurement points

vertical components of actual seismic waves such as El Centro (Imperial Valley Earthquake, 1940), Hachinohe (Tokachi-Oki Earthquake, 1978) , Tohoku University 9F (Miyagi-ken-Oki Earthquake, 1978) and simulated floor response waves based on response accelerations of single-degree-of freedom systems, whose natural frequency is 2 Hz and damping ratio is 3 %, to El Centro and Hachinohe records, were used.

Figure 4 shows a schematic view of isolated equipment and measurement points. As shown in Fig. 4, horizontal and vertical displacements and restoring forces generated in the isolation device and the horizontal and vertical accelerations of the floor, the equipment and the shaking table were measured.

3 ANALYTICAL MODEL

Supposing that the equipment is rigid body and taking sway and rocking motion into consideration, an analytical model is made as shown in Fig. 5. Analytical equations of motion are established as follows and time history response analysis is carried out using Runge-Kutta-Gill method.

Since the kinematic friction coefficient of the FPB increases with increased velocity, a velocity dependent friction coefficient assumption was also employed in the analysis. Figure 6 shows an analytical model and an experimental result of the velocity-dependent friction force characteristics of the FPB. The relative velocity of the FPB to the shaking table was derived from derivative value of displacement directly measured.

i) Lock up mode ..... Phase I

$$\ddot{x}_1 + 2\zeta_1\omega_1(\dot{x}_1 - H\dot{\phi}) + \omega_1^2(x_1 - x_0 - H\phi) = -\ddot{z}_H \quad (1)$$

$$\dot{x}_0 = 0 \text{ and } x_0 = \text{const.} \quad (2)$$

$$\ddot{\phi} - 2\xi_1\omega_1(\dot{x}_1 - H\dot{\phi})H - \Omega_1^2(x_1 - x_0 - H\phi)H + 2\xi_\phi\Omega_\phi\dot{\phi} + \Omega_\phi^2\phi = 0 \quad (3)$$

ii) Sliding mode ..... Phase II

$$\ddot{x}_1 + 2\zeta_1\omega_1(\dot{x}_1 - \dot{x}_0 - H\dot{\phi}) + \omega_1^2(x_1 - x_0 - H\phi) = -\ddot{z}_H \quad (4)$$

$$\ddot{x}_0 - 2\zeta_0\omega_0(\dot{x}_1 - \dot{x}_0 - H\dot{\phi}) - \omega_0^2(x_1 - x_0 - H\phi) + (1+\rho)\frac{g}{r}x_0 + \mu_k(1+\rho)g\cdot\mathrm{sgn}(\dot{x}_0) = -\ddot{z}_H \quad (5)$$

$$\ddot{\phi} - 2\xi_1\omega_1(\dot{x}_1 - \dot{x}_0 - H\dot{\phi})H - \Omega_1^2(x_1 - x_0 - H\phi)H + 2\xi_\phi\Omega_\phi\dot{\phi} + \Omega_\phi^2\phi = 0 \quad (6)$$

iii) Change conditions between Phase I and Phase II

a) Phase I → PhaseII

$$\left| -\ddot{z}_H + 2\zeta_0\omega_0(\dot{x}_1 - H\dot{\phi}) + \omega_0^2(x_1 - x_0 - H\phi) - (1+\rho)\frac{g}{r}x_0 \right| > \mu_s(1+\rho)g \quad (7)$$

b) Phase II → Phase I

$\dot{x}_0 = 0$ and

$$\left| -\ddot{x}_0 - \ddot{z}_H + 2\zeta_0\omega_0(\dot{x}_1 - \dot{x}_0 - H\dot{\phi}) + \omega_0^2(x_1 - x_0 - H\phi) - (1+\rho)\frac{g}{r}x_0 \right| \le \mu_s(1+\rho)g \quad (8)$$

iv) Velocity-dependent friction coefficient

1) $\mu_k = 7.14\times10^{-5}$ for $\dot{x}_0 \le 1.36\times10^{-3}$ (m/s) (9)

2) $\mu_k = 1.73\times10^{-2} + 2.80\times10^{-2}\times ln|\dot{x}_0| - 3.50\times10^{-2}\times|\dot{x}_0|$ for 1.36×10^{-3} (m/s) $< \dot{x}_0 \le 1.16$ (m/s) (10)

3) $\mu_k = 1.40\times10^{-1}$ for 1.16 (m/s) $< \dot{x}_0$ (11)

where,

$\rho = m_0/m_1$, $\omega_1^2 = k_1/m_1$, $2\zeta_1\omega_1 = c_1/m_1$, $\omega_0^2 = k_1/m_0$,

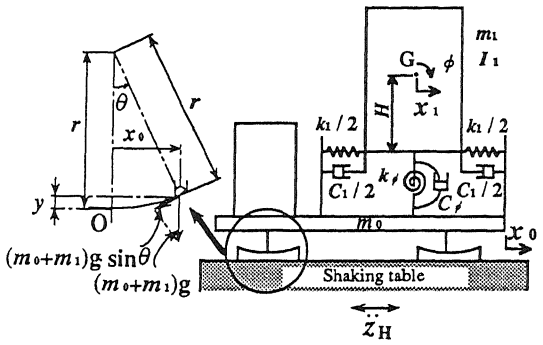

Fig. 5 Analytical model

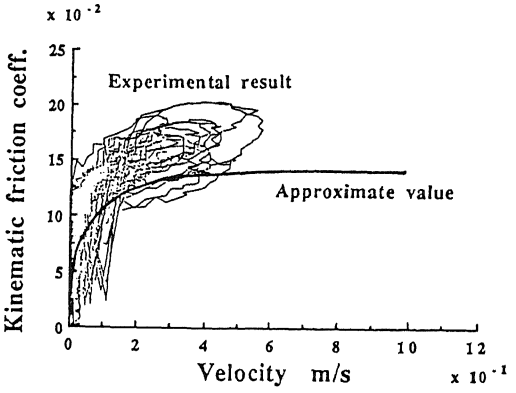

Fig. 6 Kinematic friction coefficient versus velocity

$2\zeta_0\omega_0 = c_1/m_0$, $\Omega_1^2 = k_1/I_1$, $2\xi_1\Omega_1 = c_1/I_1$, $\Omega_\phi = k_\phi/I_1$, $2\xi_\phi\Omega_\phi = c_\phi/I_1$

x_0, x_1 : relative displacements of mass points to the ground

ϕ : rotational angle of equipment on the right side of the floor

m_0 : mass of the floor including the left equipment

m_1, I_1 : mass and moment of inertia for center of gravity of the equipment on the right side of the floor

k_1, c_1 : stiffness and damping coefficient of the equipment on the right side of the floor

k_ϕ, c_ϕ : rotational stiffness and damping coefficient of the equipment on the right side of the floor

μ_k, μ_s: kinematic and static friction coefficient of the FPB

z_H : horizontal displacement of the ground

H : elevation of the center of gravity of equipment from the floor surface

r : length of radius of curvature of the FPB

g : acceleration of gravity

4 EXPERIMENTAL AND ANALYTICAL RESULTS

Figure 7 shows the results of all seismic excitation tests for maximum input of each seismic wave. For each test, the response acceleration of the equipment and the floor when isolated and non-isolated to the same input level are compared. Response displacements of the FPB are also shown together with simulation results for the isolated case to compare with the corresponding experimental results. It must be mentioned that the results when non-isolated were obtained from the results to smaller excitation, about one third of the amplitude for both directions, by linear scaling to avoid the non-isolated equipment being failed.

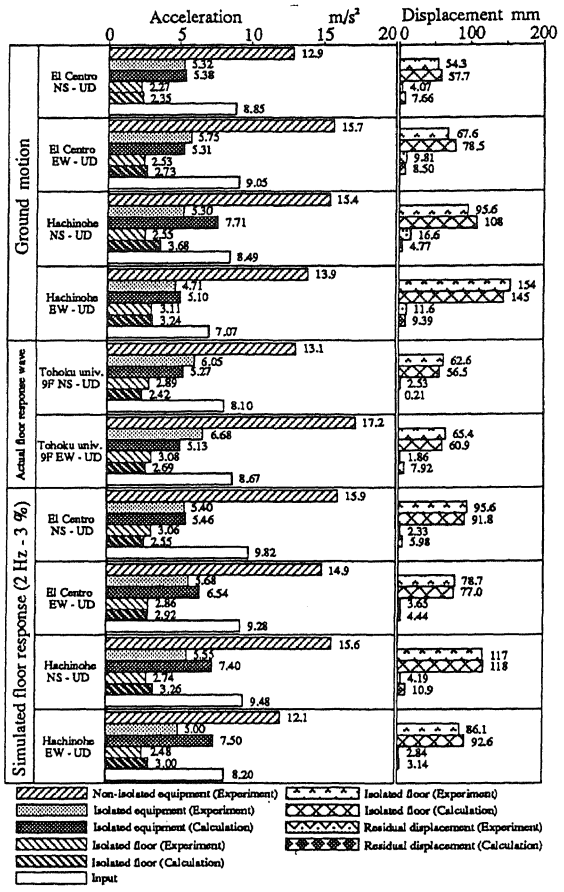

Fig. 7 Performance of earthquake isolation

The results in Fig. 7 are considered sufficient to apply the FPB to precision equipment such as computer systems. Using the FPB isolation system, the response accelerations of the floor were reduced to 25~45% of input values. And the response accelerations of the equipment were also reduced to 55~80% of input acceleration. In comparison with non-isolated conditions, the responses of the equipment under isolated condition were remarkably reduced to 30~50% of non-isolated condition. Although the residual displacements have been seen in all cases, the values of them are considered to be negligibly small for a practical use. And the results for vertical inputs are not presented in this paper, but any amplifications of vertical responses have not been found. In addition, this figure also shows the analytical results with good agreement.

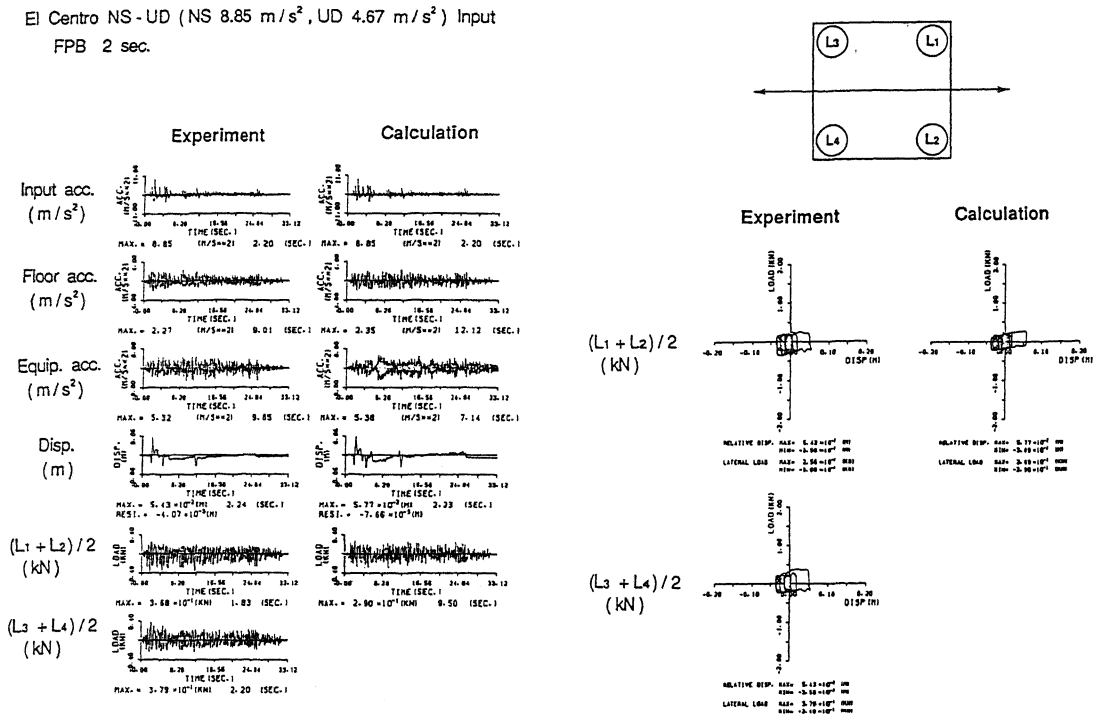

Fig. 8 Experimental and simulated time history responses and restoring force characteristics of the FPB

Figure 8 shows the experimental and the simulated time history responses of the isolated model including lateral restoring force characteristics of the FPB for El Centro NS-UD waves. The analytical results agree well with the experimental results.

5 CONCLUSIONS

It was confirmed that the isolation system using the FPB is very much effective for reducing response acceleration of equipment due to seismic excitation. And the proposed theoretical method would be applied to design the FPB, since it is effective for estimating the dynamic properties of the system with good accuracy. In addition, since the FPB for seismic isolation is very simple in its structure and considered to be easily installed to precision machinery systems as compared with the other types of isolation system/floor proposed so far, we hope it would be widely applied to many types of equipment to satisfy seismic requirements.

As a second step of research and development of the FPB, experimental tests on material characteristics will be carried out to investigate the dependencies of velocity and vertical load on kinematic friction coefficient more clearly.

ACKNOWLEDGEMENTS

The authors would like to express their appreciation to the following graduates of Tokyo Denki University, Mr. H. Obata and Mr. M. Yanagawa, for their great assistances. Acknowledgement also is due to Prof. H. Shimosaka of Meiji University for his great help.

REFERENCES

Fujita, S. 1991: *Science of machine*(in Japanese). vol.43, no.12: 1275-1282.

Simoda, I. 1990: *Component tests of bearing materials for use in friction pendulum seismic isolators*. Prepr. of Jpn. Soc. Mech. Eng (in Japanese) No.900-44: 400-403.